Determining Seasonal Termite Damage Periods in Korean Wooden Cultural Heritage Buildings Based on Temperature-dependent Wood Consumption and Activity of Subterranean Termites

Ik-Gyun Im [a,b] Kyoung-Hyun Ryu,[a] and Gyu-Seong Han [a,*]

The feeding activity of the subterranean termite *Reticulitermes speratus* was investigated under different temperature conditions. Wood consumption and microwave signal intensity increased with temperature and were highest at 21 to 27 °C. Feeding activity decreased above 30 °C, and termite movement was also reduced at high temperatures. These changes may be related to thermal stress and reduced activity of hindgut symbiotic protozoa. Field temperature data collected from wooden cultural heritage buildings and surrounding soil environments showed that temperatures suitable for termite activity were maintained from spring to autumn in many regions of Korea. Seasonal temperature changes were also associated with the overwintering and reproductive characteristics of *R. speratus*. Based on these results, installation of chitin synthesis inhibitor (CSI) bait systems in early spring may improve termite control before peak summer activity. The results of this study may be useful for termite monitoring and management of wooden cultural heritage buildings.

DOI: 10.15376/biores.21.3.8350-8365

Keywords: Wooden cultural heritage; Temperature-dependent activity; Cold hardiness; Thermal defaunation; Colony elimination

Contact information: a: Department of Wood and Paper Science, Chungbuk National University, Cheongju, 28644, Republic of Korea; b: Conservation Laboratory, Curatorial Affair Division, Gyeongju National Museum, Korea, Gyeong Ju, 38171, Republic of Korea;
** Corresponding author: wood@chungbuk.ac.kr*

INTRODUCTION

Wood is a sustainable natural resource and a core structural material for traditional wooden buildings (Han and Lee 1999). However, as an organic material, its structural stability is severely threatened by biodegradation from insects and fungi. Recent global climate change and rising average temperatures on the Korean Peninsula are accelerating this degradation in unprecedented ways (Jeong 2013). Historically, the cold and dry winter climate of the Korean Peninsula restricted the survival and reproduction of wood-boring pests (Lee *et al.* 2001). However, recent warming trends have elevated minimum winter temperatures, allowing pests that previously perished to successfully overwinter (Han and Lee 1999; Lee *et al.* 2001). Because the physiological metabolic rates of ectothermic insects accelerate exponentially with temperature (Han and Lee 1999), future climate change scenarios can be expected to rapidly expand the extent and density of biological damage to lignocellulosic resources.

The dominant wood-destroying pest causing substantial economic and cultural heritage losses in South Korea is the subterranean termite, *Reticulitermes speratus* (Han *et al.* 1998). This cold-hardy species possesses outstanding physiological adaptability, allowing it to maintain metabolic activities even in low-temperature environments without entering complete diapause (Lee and Jeong 2004; Jeong 2013). To survive harsh winters, *R. speratus* accumulates high concentrations of cryoprotectants - such as glycerol, glucose, and trehalose - and precisely regulates internal homeostasis to depress its supercooling point (Choi *et al.* 2016; Takata *et al.* 2023). Consequently, they maintain locomotor activity even below 5 °C (Fuchikawa *et al.* 2012). To evade adverse aboveground conditions, colonies progressively relocate to insulated subterranean nests beneath tree stumps or deep within the soil (Takata *et al.* 2023). They preferentially consume the cellulosic components of softwoods such as pine (*Pinus* spp.) and, due to their vulnerability to desiccation, severely degrade structurally vulnerable areas where moisture is retained, such as column bases and under-floor spaces in direct contact with the soil (Han *et al.* 1998; Jeong 2013).

The primary challenge in conserving wooden architecture against subterranean termites stems from their cryptic foraging behavior. Through constructing networks of mud tubes and galleries inside the soil or timber, they leave no distinct external signs, rendering early visual detection virtually impossible (Han *et al.* 1998). Continuous internal consumption leads to extensive cavitation, sometimes drastically reducing the timber's load-bearing capacity and risking sudden structural collapse under external stresses such as earthquakes or heavy snow. Current conservation practices rely on chemical injection, soil treatment, and baiting systems, but their timing depends on unscientific conventions. Termites are visibly exposed only during the spring swarming season when winged alates emerge. This typically occurs long after massive colonies have already heavily infested the wood. Although fragmentary data exist regarding vertical migration to evade temperature extremes, a quantitative timeline identifying when they commence and cease wood consumption in actual subterranean environments remains unestablished, leaving a lack of standard guidelines for optimal preemptive control (Han *et al.* 1998).

Termite feeding and intra-nest behaviors fluctuate in direct correlation with microclimatic variations in ambient and subterranean thermal environments (Evans and Gleeson 2001). In the southern regions of the Korean Peninsula, elevated underground winter temperatures prompt continuous concerns over year-round damage (Lee and Jeong 2004). To optimize control efficacy and minimize chemical abuse, quantitative matching studies between actual soil temperatures and termite physiological thresholds are imperatively required.

To address this gap, this study established a dual framework: First, nationwide climate data over the past 20 years (2003 to 2023) from the Korea Meteorological Administration were compiled to statistically derive seasonal thermal characteristics at a depth of 5 cm underground. Second, an environmentally controlled incubator system was utilized to screen the quantitative wood consumption rate and absolute locomotor activity of *R. speratus* across a temperature spectrum from -3 to 36 °C through laboratory bioassays. Through mapping these laboratory physiological profiles against multi-year regional subterranean temperature data, this study aimed to quantitatively estimate the annual risk periods during which termites resume and cease activity. Such findings can provide critical scientific baseline data to establish season-specific pest control guidelines for field conservation practices. Unlike previous laboratory studies that primarily defined thermal activity thresholds of *R. speratus*, the present study integrated wood consumption,

microwave-based activity monitoring, morphological damage assessment, nationwide soil-temperature datasets, and wooden cultural heritage microclimate monitoring into a management-oriented framework for termite risk assessment.

EXPERIMENTAL

Termite Collection

Subterranean termites were sampled from naturally infested wooden logs located within the campus forest of Chungbuk National University and its adjacent suburban experimental forest. These colony-containing logs were transported and maintained under controlled laboratory conditions. To minimize colony disturbance and avoid mechanical damage to the insects, termites were extracted using a non-destructive transfer method modified from Im and Han (2021); the individuals were allowed to voluntarily migrate from the logs into moistened cardboard scrolls.

Experimental Setup and Bioassay Design

Wood specimens prepared from *Pinus* spp. were cut into dimensions of 20 mm (T) × 20 mm (R) × 10 mm (L). Prior to the bioassay, the specimens were submerged in distilled water for 24 h to ensure sufficient moisture absorption, and excess surface water was gently removed immediately before the experiment. Cylindrical glass vials (40 mm in diameter, 80 mm in height) were utilized as testing chambers, each featuring a 6-mm diameter access hole drilled at a height of 30 mm from the base. To maintain adequate internal humidity during the testing period, a matrix consisting of silica sand and vermiculite mixed at a 7:6 (w/w) ratio was formulated, following the protocol adapted from Lee and Forschler (2016). After sterilization, 40 g of this composite substrate was introduced into each vial, filling it up to the level of the 6-mm access hole to facilitate the seamless movement of termite workers. The experimental apparatus comprised a dual-chamber system where two identical cylindrical vials were interconnected using a plastic tube (100 mm in length, 4 mm in internal diameter). For the bioassay configuration, 150 termite workers were released into the left vial (designated as the termite chamber), while a single pre-conditioned wood specimen was placed in the right vial (designated as the wood chamber) (Fig. 1). To ensure environmental adaptation, the interconnecting tube was initially blocked for the first 24 h. This acclimation period allowed the introduced workers to stabilize within the termite chamber by initiating active tunneling behavior throughout the substrate. Following the 24-h stabilization period, the connection between the two chambers was opened, allowing the termites access to the wood specimen chamber, and the bioassay was conducted for one week. Each experimental condition consisted of five replicates and was repeated three times.

Non-destructive Evaluation of Termite Activity and Signal Quantification

To detect temperature-dependent termite activity non-destructively, a microwave-based detection device (Termatrac T3i; Termatrac Co., Australia) was employed following the operational protocol described by Im and Han (2022). The sensor unit of the device was placed in direct contact with the upper surface of the airtight lid sealing the wood chamber. To evaluate the maximum detection capabilities of the system, the signal amplification was set to its highest level (Gain: 10). Real-time detection data were synchronized and monitored *via* the Termatrac T3i application (ver. 3.38) installed on a

smartphone (Galaxy S10 5G, SM-G977N; Samsung, Korea). In accordance with the manufacturer's guidelines, an initialization and self-calibration window of 15 to 20 s was allowed immediately after activating the device to baseline the measurement values. Following this stabilization period, the real-time application screen displaying the radar graph was captured *via* automated screenshots at 15-s intervals and subsequently transferred to a personal computer for digital analysis.

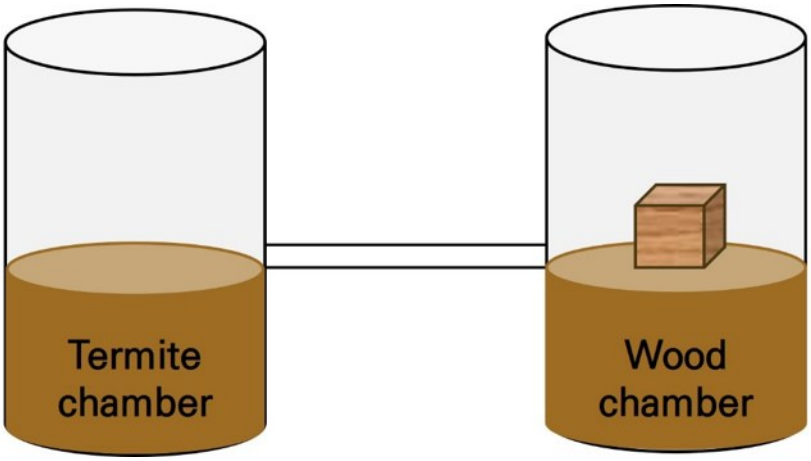

Fig. 1. Schematic diagram of the dual-chamber bioassay apparatus. The experimental setup consists of two cylindrical vials (Ø 40 mm × 80 mm) sealed with airtight lids to maintain internal humidity. The chambers are interconnected by a plastic tube (100 mm in length, 4 mm i.d.). The "Termite chamber" contained 150 *R. speratus* workers introduced onto a sterile silica sand and vermiculite substrate (7:6 w/w). The "Wood chamber" contained a single pre-conditioned wood specimen (20 mm × 20 mm × 10 mm) placed on the same substrate level with the 6-mm access hole to facilitate termite foraging activity.

The signal intensity within the captured radar graph domain was quantified utilizing digital image processing software (Adobe Photoshop CC 2017). To calculate the integral values of the activity waves, the area beneath the radar curve was isolated using the Rectangular Marquee Tool and subsequently filled with a solid blue color (Hex color code: #0000ff) using the Paint Bucket Tool. The color-coded area under the curve was then selected with the Magic Wand tool, and its cumulative surface area was computed in square pixels *via* the 'Measurement Log' history panel. This pixel density value was utilized as a quantitative index to benchmark the Termatrac T3i signal intensity across the different experimental conditions. For each temperature regimen, ten replicate screenshots were evaluated to determine the representative mean signal intensity.

To determine the statistical significance of the differences among the experimental groups, a one-way analysis of variance (ANOVA) was performed using SPSS software (ver. 26; IBM Corp., Armonk, NY, USA), followed by Tukey's honestly significant difference (HSD) test as a *post-hoc* analysis for multiple comparisons.

Analysis of Subterranean and Wooden Cultural Heritage Thermal Environments

Subterranean thermal environments were characterized using a 20-year dataset (2003 to 2023) of monthly mean soil temperatures obtained from the Korea Meteorological Administration (KMA). Temperatures were evaluated at depths of 5 cm – the primary foraging zone for subterranean termites – and 30 cm to capture regional and seasonal

dynamics. These data served as a baseline profile for ambient soil temperatures across the Korean Peninsula.

To evaluate the real-world thermal behavior of historical wooden structures, five wooden cultural heritage (WCH) buildings located across different regions in Korea were selected as study sites to monitor internal temperatures (Table 1). Indoor and outdoor temperature of these WCHs were continuously recorded from 2021 to 2023 using a wireless real-time monitoring (RTM) system (Im *et al.* 2021; Im and Han 2025). The resulting monthly mean temperatures were cross-analyzed with the 5 cm and 30 cm subterranean temperature datasets to determine microclimatic correlations and structural thermal lags.

Table 1. Geographical and Structural Characteristics of the Five Selected WCHs in Korea

No.	Region		Temple	Latitude and Longitude		Wooden Cultural Property
1	Gyeong-gi	Yangju	Cheongnyeongsa	37.7299	126.9480	Daeungjeon Hall
2	Chung-buk	Cheongju	Ansimsa	36.5522	127.4130	Daeungjeon Hall
3	Gyeong-buk	Gimcheon	Jikjisa	36.1164	128.0038	Daeungjeon Hall
4	Jeon-nam	Gangjin	Muwisa	34.7384	126.6868	Geungnakbojeon Hall
5		Yeosu	Heongguksa	34.8211	127.7003	Daeungjeon Hall

These field-monitored thermal profiles were then compared against the temperature-dependent feeding capacity and behavioral thresholds of *R. speratus* obtained from laboratory bioassays. The critical foraging activation range, which spans from initial activity acceleration to peak wood consumption, was defined as the high-risk threshold. Mapping the monthly structural and soil temperatures onto this biological activity matrix allowed for the quantification of temporal overlaps, identifying specific periods of elevated risk for termite damage in WCHs.

RESULTS

Temperature-dependent Wood Consumption Rates and Microwave Signal Intensities

The integration of quantitative mass loss data (Fig. 2), the qualitative morphological matrix of all replicates (Fig. 3), and non-destructive microwave signal intensities (Fig. 4) revealed a synchronized, non-linear thermal response in the foraging behavior and metabolic movement of *R. speratus*. The thermal spectrum evaluated over the bioassay period can be categorized into four distinct behavioral and structural damage zones, verified concurrently by physical degradation and electromagnetic activity tracking.

Critical low-temperature zone (-3 °C to 9 °C): Complete foraging and movement suppression

In the critical low-temperature range spanning from -3 °C to 9 °C, wood consumption by *R. speratus* was statistically negligible, with mean mass loss values remaining near 0 mg (Fig. 2). All treatments within this window were statistically grouped into the same homogeneous cluster ($P \geq 0.05$). This arrest of foraging activity was

corroborated by the microwave sensor data (Fig. 4), where the signal strength at -3 °C and 0 °C remained at baseline levels, displaying no statistically meaningful difference from the inactive state (*a*, $P \geq 0.05$). Although a slight statistical transition in signal intensity occurred at 3 °C and 6 °C (*b*) and reached cluster *c* at 9 °C, this minor movement did not translate into effective feeding. Visual examination of the 25 specimens validated this trend; the wood blocks preserved their sharp geometric edges and original cuts (Fig. 3), indicating that sub-10 °C conditions induce a state of cold stupor that deactivates mechanical shredding behavior despite minor basal movements at the upper edge of this zone.

Activity initiation and transition window (12 °C to 18 °C): Stepwise damage acceleration

A statistical threshold was breached as the temperature advanced to the activity initiation and transition window of 12 °C to 18 °C. At 12 °C, the mean wood consumption escalated to approximately 0.07 mg, separating into a distinct statistical group (*b*, $P < 0.05$). This physical onset of feeding was driven by a parallel surge in locomotion, as the microwave signal intensity established an active profile within cluster *c* across the 12 to 18 °C spectrum ($P < 0.05$). As incubation temperatures progressed to 15 and 18 °C, mass loss values exhibited a steady, stepwise increase, transitioning sequentially into statistical clusters *bc* and *c*, respectively. Morphologically, a corresponding gradient of structural deterioration emerged across all replicates; initial damage manifested as a slight rounding of the block corners at 12 °C, while the parallel replicates at 15 °C and 18 °C synchronously displayed distinct, shallow longitudinal grooves (Fig. 3), confirming that the worker population initiated active, directed mechanical shredding facilitated by coordinated physical movement within this transitional window.

Optimal thermal zone (21 to 27 °C): Severe structural collapse and peak locomotion

The maximum wood-degradation capacity and physical locomotion of *R. speratus* were concentrated within the mesophilic optimal thermal zone of 21 to 27 °C. The wood consumption treatments within this range formed the highest statistical cluster (*d*, $P < 0.05$), with the peak of destruction recorded at 27 °C where the mean mass loss reached approximately 0.25 mg. This wood degradation was synchronized with the peak biological activity captured *via* non-destructive sensing; the microwave signal strength surged, reaching its apex at 24 and 27 °C to form the highest statistical group (*d*, $P < 0.05$). The visual matrix for the 21 to 27 °C groups demonstrated severe structural failure across all parallel trials, characterized by internal cavitation and hollowed-out cores. Crucially, the degradation pattern exhibited a distinct earlywood-preference feeding behavior, where worker termites excavated the softer earlywood bands while leaving the denser latewood lines intact, giving the replicates at 27 °C a striated, skeletal appearance (Fig. 3), showing that peak structural hazard coincides with the period of maximum behavioral movement.

High-temperature inhibition zone (30 to 36 °C): Abrupt behavioral and locomotor arrest

Conversely, when the incubation temperature was raised to the high-temperature inhibition zone (30 °C to 36 °C), an abrupt decline was observed in both feeding and movement. The mean wood mass loss declined from the 27 °C peak down to approximately 0.065 mg at 30 °C (*bc* cluster), rendering it statistically indistinguishable from the low-activity baseline at 15 °C. This behavioral suppression was validated by the microwave data (Fig. 4), where the signal intensity decreased at 30 °C (cluster *c*) and fell further at 33 °C (*b*), culminating in locomotor cessation at 36 °C, which returned to the inactive baseline

group (*a*). This suppression of damage was apparent in the visual matrix; the replicates incubated at 30 °C remained structurally stable, exhibiting only superficial etching and minor localized abrasions (Fig. 3). This provides morphological and electromagnetic evidence that temperatures exceeding 30 °C induce thermal stress, mitigating the mechanical wood-shredding capacity of the worker population *via* suppression of biological activity. A similar pattern was observed in termite survival (Fig. 5). Worker mortality remained relatively low between 0 °C and 30 °C, but increased sharply under extreme temperature conditions. In particular, mortality rapidly increased at 33 °C and reached its highest level at 36 °C, indicating that the observed reduction in feeding and locomotion at elevated temperatures was not solely associated with behavioral avoidance, but also reflected physiological stress approaching the upper thermal tolerance limit of the worker caste.

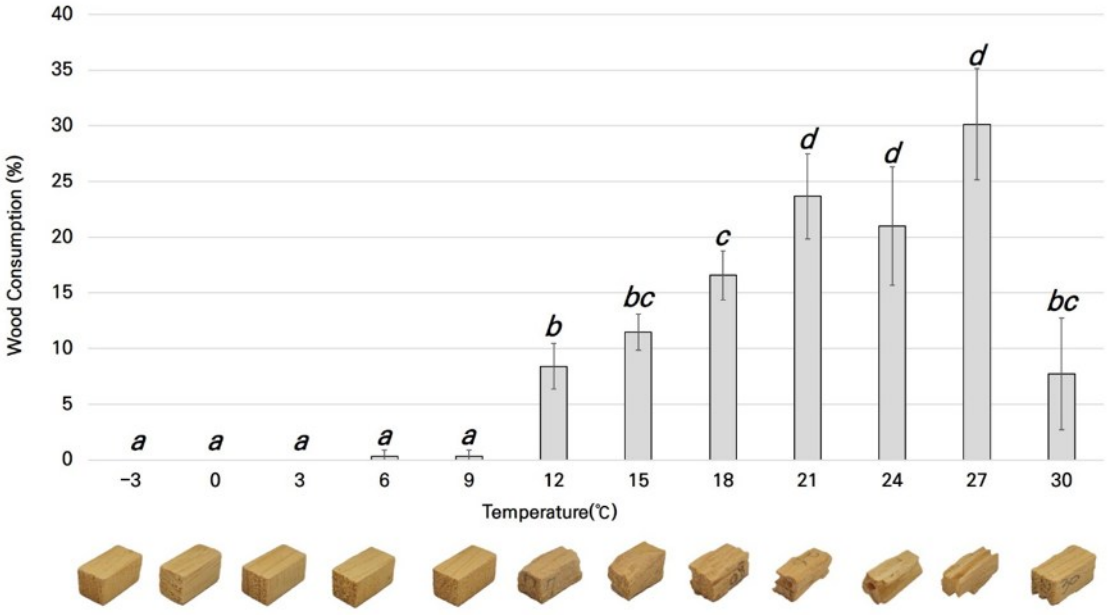

Fig. 2. Temperature-dependent wood consumption rates and visual degradation profiles of *R. speratus*

The bar graph illustrates the mean mass loss (mg) of wood specimens subjected to a wide thermal spectrum ranging from -3 to 30 °C over a one-week bioassay period. Error bars represent the standard error of the mean (SEM). Different lowercase letters (*a* to *d*) above the bars indicate statistically significant differences between experimental temperature groups based on One-way ANOVA followed by Tukey's honestly significant difference (HSD) test ($P < 0.05$). The macro-photographs aligned below the x-axis display the corresponding physical degradation and macro-structural deterioration of the wood specimens at each designated temperature condition.

The image portfolio systematically displays the entire set of five experimental replicates for each designated temperature regimen, spanning from -3 to 30 °C. Minimal to zero structural alteration was observed between -3 and 9 °C, whereas progressive gallery formation, surface channeling, and substantial mass reduction become visually prominent from 12 °C upward, reaching a peak of structural collapse at 27 °C.

Fig. 3. Macro-photographic matrix of all replicated wood specimens after a one-week termite feeding assay

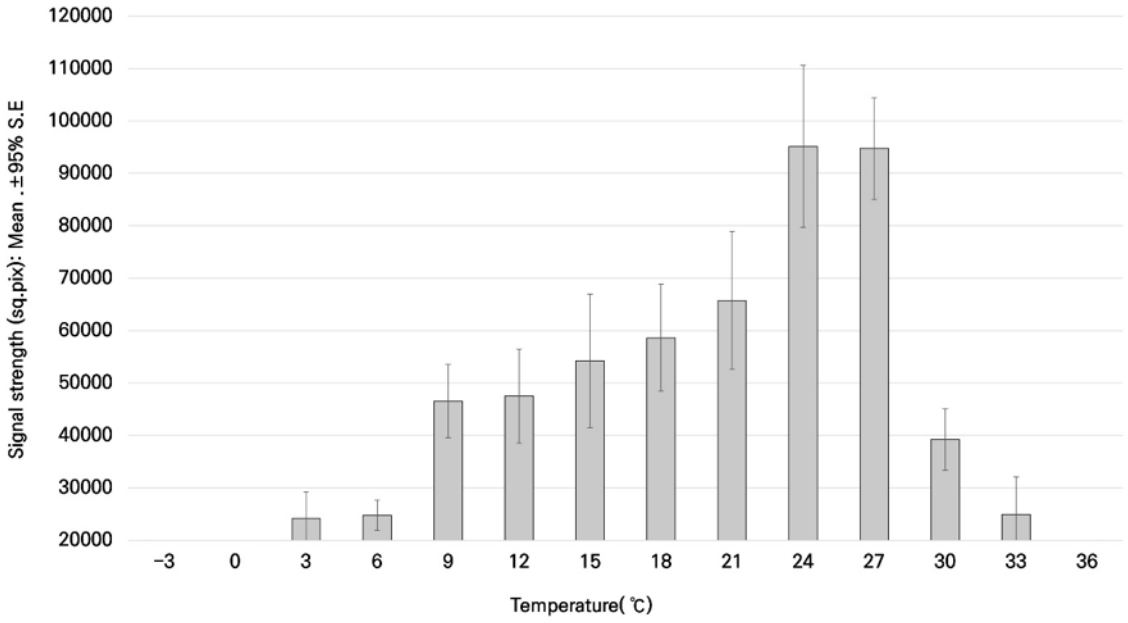

Fig. 4. Temperature-dependent microwave signal intensities of *R. speratus* activity; The bar graph displays the mean signal strength (sq. pix) with ± 95 sampling error (S.E.) bars across a thermal gradient from -3 °C to 36 °C. Different lowercase letters (*a* to *d*) indicate statistically significant differences between temperature groups based on One-way ANOVA followed by Tukey's HSD test ($P < 0.05$).

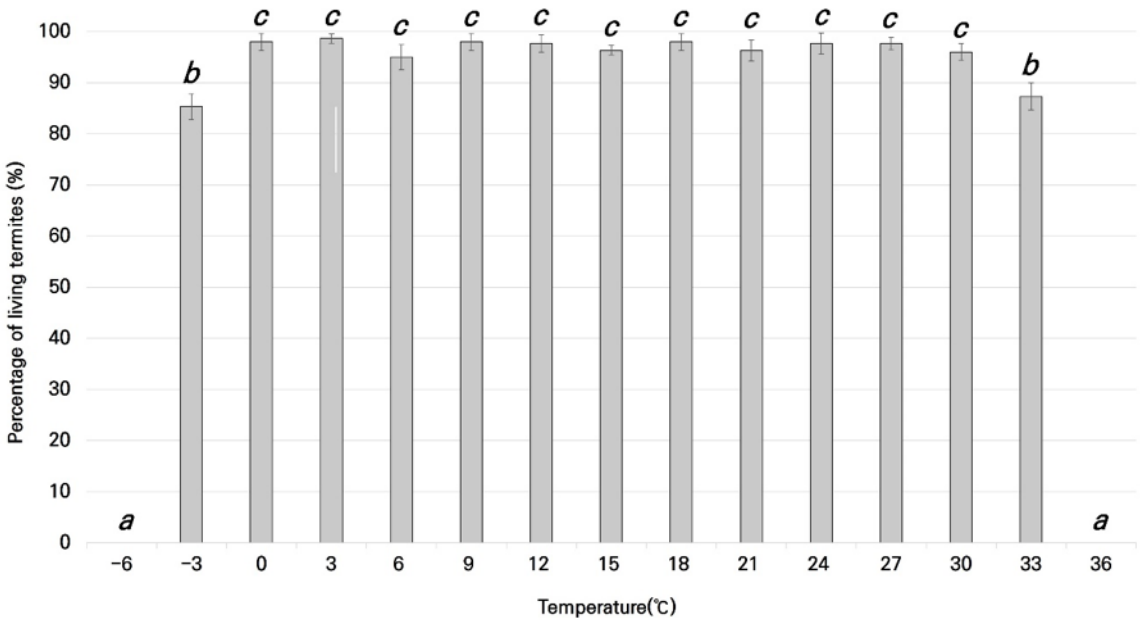

Fig. 5. Mortality of *R. speratus* workers under different temperature conditions after a one-week exposure period. Error bars represent standard deviations. Different lowercase letters indicate significant differences among temperature conditions according to Tukey's HSD test ($P < 0.05$).

Overlap Analysis of Field Environmental Profiles and Termite Thermal Thresholds

The comparison between the 20-year subterranean temperature baseline (2003 to 2023), the field-monitored WCH structural temperatures (2021 to 2023), and the laboratory-derived biological thresholds (12 to 27 °C) established the precise seasonal window for subterranean termite hazards (Fig. 6). Environmental profiles showed a clear seasonal transition where internal, external, and soil temperatures converged into and diverged from the biological risk matrix throughout the annual cycle.

From November to March, all measured microclimatic parameters - including WCH indoor/outdoor structural components and both subterranean layers (5 cm and 30 cm) - remained below the 12 °C activity initiation threshold. During this period, minimum temperatures were recorded between December and February, with KMA soil-temperature records indicating that the 5 cm subterranean layer fell near or below 0 °C in northern regions such as Cheorwon and Chuncheon. Although the 30 cm subterranean layer exhibited a structural thermal lag that insulated it against rapid ambient freezing, its monthly means still stayed under 5 °C during the winter season, consistently indicating a state of complete behavioral suppression for *R. speratus*.

Conversely, a critical thermal transition occurred in April, where the monthly mean temperatures of WCH indoor and outdoor components rose to approximately 15 °C, entering the high-risk activity window (Fig. 6). It is worth mentioning that during this initiation phase, the 5 cm and 30 cm subterranean temperatures lagged slightly behind the structural members, hovering near the lower boundary of the risk zone at 12 to 13 °C. From May through September, a prolonged thermal overlap was established as all monitored structural and soil elements shifted into the high-risk thermal matrix (12 to 27 °C).

The environmental profiles peaked during July and August. In July, WCH indoor and outdoor temperatures reached approximately 27 °C, aligning with the maximum wood-consumption capacity determined in the bioassay. Concurrently, the subterranean 5 cm and

30 cm temperatures remained within the optimal activity zone, varying between 23 °C and 26 °C. While regional variations existed in the KMA dataset – such as Jeju maintaining elevated subterranean temperature baselines year-round compared to inland locations such as Cheorwon – the collective nationwide data confirmed that the high-risk damage period spans uninterrupted for six months, from April to October. The hazard window terminated in October, where a downward thermal transition shifted WCH outdoor and subterranean elements toward the lower limit of the risk threshold, preceding the complete cessation observed in November.

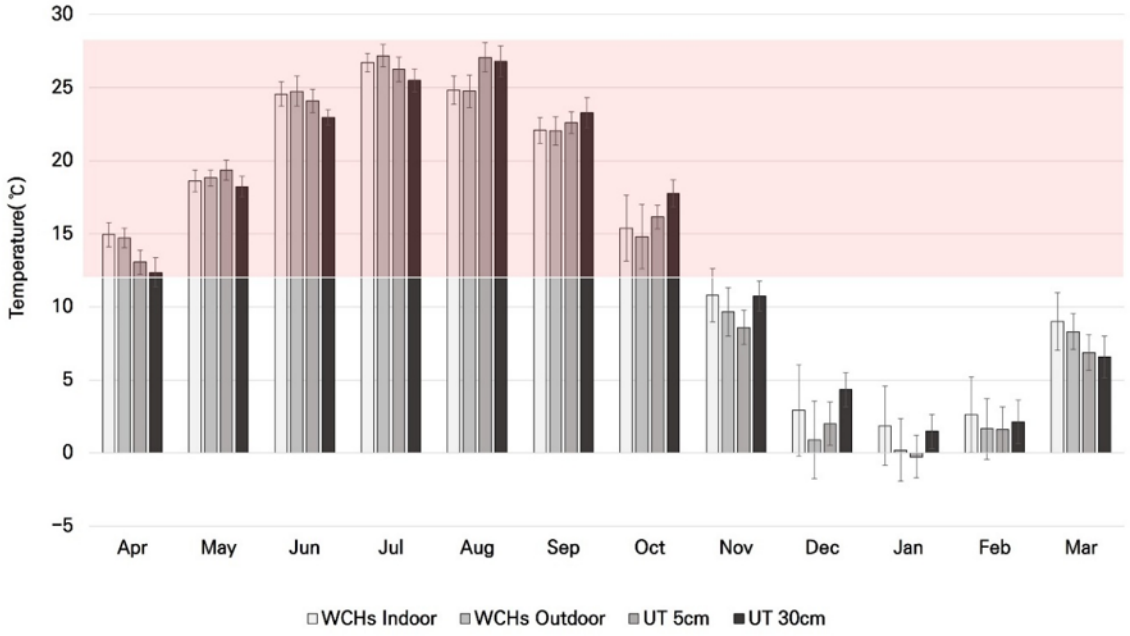

Fig. 6. Seasonal variations in the monthly mean temperatures of wooden cultural heritages (WCHs indoor and outdoor) and subterranean environments (UT 5 cm and 30 cm). The shaded red matrix defines the high-risk thermal threshold (12 °C to 27 °C) derived from the *R. speratus* laboratory bioassay. Error bars indicate the standard deviation of monitored temperature variations across the studied regions.

DISCUSSION

Cold Hardiness Mechanisms and Seasonal Colony Movement (< 12 °C)

The laboratory-derived thermal responses of *R. speratus* align with field microclimatic profiles, indicating that colony survival and foraging kinetics are governed by seasonal temperature fluctuations. Unlike many temperate insects that enter diapause below 5 °C, *R. speratus* maintains basal metabolic activity at low temperatures, demonstrating pronounced cold hardiness (Fuchikawa *et al.* 2012). This physiological resilience supports colony persistence even when the 5 cm soil depth drops to approximately -3 °C in January (Fig. 6).

Seasonal migration further enhances winter survival. Founding kings and queens inhabit above-ground decayed wood during the active foraging period (May to October), but they retreat to dedicated subterranean royal chambers within stump root systems in autumn. Empirical data show that mortality accelerates significantly below -8 °C for reproductives and below -4 °C for workers and soldiers, with estimated *LT50* values of -

8.0 °C and -6.4 °C to -6.6 °C, respectively (Takata *et al.* 2023). Subterranean royal chambers and above-ground logs provide thermal buffering of 6.0 °C and 0.3 °C, respectively, mitigating lethal cold exposure. Because primary reproductives require over five years to establish high-capacity oviposition *via* secondary neotenics, surviving multiple winters is critical for long-term colony stability (Matsuura *et al.* 2004, 2007; Kawatsu and Matsuura 2013; Matsuura and Kobayashi 2010). These overwintering adaptations are foundational parameters for modeling subterranean termite distribution and persistence under shifting climate regimes.

Nutritional Dynamics, Fungal Interactions, and Reproductive Synchronization (12 to 27 °C)

The prolonged annual overlap between field microclimates and the optimal temperature range (12 to 27 °C; Fig. 5) corresponds directly to the reproductive phenology of *R. speratus*. While temperature strongly influences egg production, seasonal oviposition kinetics are not driven solely by ambient heat. Matsuura *et al.* (2007) noted that daily egg production rates (EPR) peak in early July, preceding the maximum atmospheric temperatures observed in August (Fig. 6). Given the 35-day incubation period of *R. speratus* eggs (Matsuura and Kobayashi 2006), this oviposition schedule ensures peak larval eclosion during August.

This temporal strategy matches the maximum feeding and wood consumption efficiency recorded at 27 °C in this study (Fig. 2). Early-instar larvae are incapable of independent feeding and rely entirely on worker trophallaxis, imposing significant nutritional demands on the colony (Matsuura *et al.* 2007). Thus, the elevated wood consumption and microwave signal intensities recorded between 21 and 27 °C (Figs. 2 and 4) reflect a coordinated colony-level response to meet the metabolic demands of brood care and midsummer population expansion.

Symbiotic Disruption and High-temperature Inhibition (> 30 °C)

The decline in wood consumption and microwave signal intensities between 30 and 36 °C cannot be explained solely by behavioral avoidance of heat. *R. speratus* relies obligatorily on hindgut cellulolytic flagellates and associated bacterial microbiota for cellulose digestion, and these endosymbionts are highly sensitive to thermal stress (Hongoh *et al.* 2003). In *Reticulitermes*, hindgut protozoan populations decline precipitously or disappear entirely above 32 °C (Smythe and Williams 1972; Belitz and Waller 1998). This thermal defaunation impairs lignocellulose digestion, inducing functional starvation and a subsequent drop in foraging activity.

Furthermore, temperatures approaching 36 °C exceed the physiological tolerance limits of the workers, triggering rapid desiccation, membrane destabilization, and heat-shock responses that compromise survivorship (Nakayama *et al.* 2004). Consistent with these physiological responses, worker mortality increased markedly under both low- and high-temperature conditions, whereas relatively low mortality was maintained between 0 and 30 °C (Fig. 5).

Practical Implications for Termite Control and Baiting Stratagems

These temperature-dependent activity thresholds, combined with field microclimatic monitoring, indicate that the efficacy of termite management depends heavily on seasonal and structural variations. As illustrated in Fig. 6, the indoor/outdoor microclimates of WCHs and soil temperatures at 5 cm and 30 cm depths remain within the

active range (12 to 27 °C) for most of the year, confirming that *R. speratus* foraging in Korea extends from early spring through autumn.

Colony elimination systems utilizing chitin synthesis inhibitor (CSI) baits are standard practice for protecting WCH structures. Early field trials demonstrated successful colony eradication and territorial suppression using bait matrices against *R. speratus* (Tsunoda *et al.* 1998). Modern CSI baits, particularly noviflumuron and novaluron achieve total colony elimination even with limited initial forager recruitment because the toxicant is distributed throughout the nest hierarchy *via* trophallaxis (Chouvenc and Su 2017; Chouvenc 2021; Gordon *et al.* 2022; Su *et al.* 2023).

However, CSI systems require a lag phase; foragers must first locate and recruit to the stations. Bait interception can take several weeks to months, followed by an additional 6 to 8 weeks for complete colony collapse *via* toxicant transmission (Im and Han 2023). Deploying bait stations before foraging and trophallactic behaviors peak can optimize eradication efficiency.

The recommendation for early spring deployment is supported not only by the temperature-dependent feeding activity observed in the present study, but also by the seasonal biology of *R. speratus*. Colonies resume foraging following overwintering, and bait interception requires sufficient time before the period of maximum colony growth, brood production, and summer feeding activity. Therefore, early-season installation may increase the probability of toxicant distribution throughout the colony before peak reproductive and nutritional demands occur.

Field profiles (Fig. 6) show that temperatures exceed the 12 °C threshold in late March to early April, marking the onset of post-overwintering activity. When temperatures transition into the optimal 21 to 27 °C range in early summer, feeding and trophallaxis accelerate. Deploying colony elimination systems between March and early April – prior to peak consumption in July and August – maximizes bait interception and toxicant transfer. However, because foraging range and bait discovery are governed by soil moisture, colony biomass, local food competition, and structural architecture, optimal installation windows should be calibrated to site-specific conditions.

Importantly, the microclimatic data in this study reflect ambient and soil temperature profiles near WCHs rather than internal temperatures within structural timbers. Because large wooden members possess substantial thermal inertia, internal timber temperatures may exhibit considerable thermal lag relative to ambient air and shallow soil environments and may therefore remain lower than ambient temperatures during summer and higher during winter, depending on timber thickness, moisture content, solar orientation, and ventilation conditions. Therefore, although direct solar radiation may elevate the surface temperature of exposed wooden members above 30 °C and locally suppress termite activity, caution is required when extrapolating these findings to the internal thermal conditions of structural timbers.

Nevertheless, the proposed seasonal guideline for CSI bait deployment may remain ecologically relevant because colony elimination systems are typically installed in soil environments adjacent to wooden structures. In this respect, the 5-cm soil temperature profiles used in the present study may provide a more directly applicable indicator of seasonal foraging activity and bait interception probability than the thermal conditions within exposed timber members themselves. The transition of soil temperatures above the 12 °C activity threshold during late March and early April therefore supports the ecological rationale for early-season bait installation.

In conclusion, colony elimination strategies targeting *R. speratus* under Korean climatic regimes are optimized when initiated in early spring. Furthermore, because subterranean microclimates provide thermal buffering that maintains partial colony activity during seasonal extremes, a temporary reduction in visible above-ground foraging should not be misinterpreted as complete colony eradication.

CONCLUSIONS

1. The foraging activity and wood consumption of the subterranean termite *Reticulitermes speratus* exhibit a distinct, non-linear thermal response, with mechanical wood degradation and locomotor movement being completely suppressed in the critical low-temperature zone from -3 to 9 °C.
2. The initiation of feeding and mechanical wood shredding breaches a statistical threshold in the transitional window of 12 to 18 °C, as corroborated by a synchronized, stepwise acceleration in both physical mass loss and non-destructive microwave signal intensities.
3. The maximum wood-degradation capacity and physical locomotion of *R. speratus* are concentrated within the mesophilic optimal thermal zone of 21 to 27 °C, reaching a peak of structural destruction and severe earlywood-preference cavitation at 27 °C.
4. Ambient temperatures exceeding 30 °C (30 to 36 °C) induce severe thermal stress and locomotor arrest, causing an abrupt decline in feeding activity that returns to the low-activity baseline, which is attributed to potential thermal defaunation of hindgut endosymbionts and physiological tolerance limits.
5. Multi-year field microclimatic mapping confirms that nationwide environmental temperatures in South Korea maintain a prolonged, uninterrupted six-month overlap (from April to October) with the high-risk biological activity threshold (12 °C to 27 °C) of *R. speratus*.
6. To optimize the eradication efficiency of chitin synthesis inhibitor (CSI) colony elimination systems, bait deployment should be strategically timed with the ecological onset of post-overwintering activity during the early spring transition window in late March to early April, prior to peak midsummer consumption.

ACKNOWLEDGEMENTS

The authors used ChatGPT (OpenAI) for English language editing and sentence refinement during manuscript preparation. All scientific interpretation, analysis, and conclusions were reviewed and verified by the authors.

REFERENCES CITED

Belitz, L. A., and Waller, D. A. (1998). "Effect of temperature and termite starvation on phagocytosis by protozoan symbionts of the eastern subterranean termite *Reticulitermes flavipes* Kollar," *Microbial Ecology* 36(2), 175-181.

Choi, B. Y., Itakura, S., and Yoshimura, T. (2016). "Do northern populations of *Reticulitermes speratus* (Kolbe) possess an additional physiological capacity to cold-acclimate that enhances cold tolerance during the winter?," *Journal of Asia-Pacific Entomology* 19(3), 643-649.

Chouvenc, T. (2021). "Subterranean termite (*Coptotermes gestroi* (Blattodea: Rhinotermitidae)) colony elimination through exposure to a novaluron CSI bait formulation in laboratory," *Journal of Economic Entomology* 114(3), 1249-1255. https://doi.org/10.1093/jee/toab061

Chouvenc, T., and Su, N. Y. (2017). "Subterranean termites feeding on CSI baits for a short duration still results in colony elimination," *Journal of Economic Entomology* 110(6), 2534-2538.

Evans, T. A., and Gleeson, P .V. (2001). "Seasonal and daily activity patterns of subterranean, wood-eating termite foragers," *Australian Journal of Zoology* 49, 311-321. https://doi.org/10.1071/ZO00083

Fuchikawa, T., Matsubara, K., Miyatake, T., and Matsuura, K. (2012). "Acoustic emission monitoring of the effect of temperature on activity rhythms of the subterranean termite *Reticulitermes speratus*," *Physiological Entomology* 37(3), 303-308. https://doi.org/10.1111/j.1365-3032.2012.00841.x

Gordon, J. M., Velenovsky, J. F., and Chouvenc, T. (2022). "Subterranean termite colony elimination can be achieved even when only a small proportion of foragers feed upon a CSI bait," *Journal of Pest Science* 95, 1207-1216.

Han, S. H., and Lee, K. S. (1999). "Preservation environment of organic cultural heritage and insect/fungal damages," *Heritage: History and Science* 32, 203-242.

Han, S. H., Lee, G. S., and Jeong, Y. J. (1998). "Characteristics and control of termites inhabiting Korea," *Conservation Studies* 19, 133-158.

Hongoh, Y., Ohkuma, M., and Kudo, T. (2003). "Molecular analysis of bacterial microbiota in the gut of the termite *Reticulitermes speratus*," *FEMS Microbiology Ecology* 44(2), 231-242.

Im, I. G., and Han, G. S. (2021). "Selection of dye markers for monitoring *Reticulitermes speratus* and identification of colonies by heterogeneous dye-marking," *Journal of the Korean Wood Science and Technology* 49(5), 514-534. https://doi.org/10.5658/WOOD.2021.49.5.514

Im, I. G., and Han, G. S. (2022). "Characteristics of detection performance changes of Termatrac T3i as a subterranean termite detection device according to wood species, moisture content, detection depth, and direction," *Journal of Conservation Science* 38(5), 549-557. https://doi.org/10.12654/JCS.2022.38.5.15

Im, I. G., and Han, G. S. (2023). "Changes over time in activity patterns of *Reticulitermes speratus* (Blattodea: Rhinotermitidae) fed fast- or slow-acting termiticides," *BioResources* 18(1), 131-142. https://doi.org/10.15376/biores.18.1.131-142

Im, I. G., and Han, G. S. (2025). "Risk of damage inside wooden cultural heritage sites based on temperature, humidity, and airborne fungi in South Korea," *BioResources* 20(1), 1838-1858. https://doi.org/10.15376/biores.20.1.1838-1858

Im, I. G., Lim, S. D., and Han, G. S. (2021). "Real-time monitoring of temperature and relative humidity and visualization of pest survey data for integrated pest management in collection storage area," *Journal of Conservation Science* 37(5), 440-450.

Jeong, S. Y. (2013). "Study of the present situation on the termite control of wooden structures(II) - Focused on the case of Japan," *Conservation Studies* 34, 84-99.

Kawatsu, K., and Matsuura, K. (2013). "Preadaptation for parthenogenetic colony foundation in subterranean termites *Reticulitermes* spp. (Isoptera: Rhinotermitidae)," *Journal of Ethology* 31, 123-128. https://doi.org/10.1007/s10164-012-0356-7

Lee, G. S., and Jeong, S. Y. (2004). "Ecolological characteristics of termite (*Reticulitermes speratus kyushuensis*) for preservation of wooden cultural heritage," *Heritage: History and Science* 37, 327-348.

Lee, G. S., Jeong, S. Y., and Chung, Y. J. (2001). "Termite monitoring and control managements for wooden building," *Conservation Studies* 22, 41-52.

Lee, T. Y., and Forschler, B. T. (2016). "Wood preference of *Reticulitermes virginicus* (Blattodea: Rhinotermitidae) using no-, two-, and four-choice designs and seven different measures of wood consumption," *Journal of Economic Entomology* 109(2), 785-791. https://doi.org/10.1093/jee/tov391

Matsuura, K. (2018). "A genomic imprinting model of termite caste determination: Not genetic but epigenetic inheritance influences offspring caste fate," *The American Naturalist* 191(6), 677-690. https://doi.org/10.1086/697238

Matsuura, K., and Kobayashi, N. (2006). "Size, hatching rate, and hatching period of sexually and asexually produced eggs in the facultatively parthenogenetic termite *Reticulitermes speratus* (Isoptera: Rhinotermitidae)," *Applied Entomology and Zoology* 42(2), 241-246. https://doi.org/10.1303/aez.2007.241

Matsuura, K., and Kobayashi, N. (2010). "Termite queens adjust egg size according to colony development," *Behavioral Ecology* 21(5), 1018-1023. https://doi.org/10.1093/beheco/arq101

Matsuura, K., Fujimoto, M., and Goka, K. (2004). "Sexual and asexual colony foundation and the mechanism of facultative parthenogenesis in the termite *Reticulitermes speratus* (Isoptera: Rhinotermitidae)," *Insectes Sociaux* 51(4), 325-332. https://doi.org/10.1007/s00040-004-0746-0

Matsuura, K., Kobayashi, N., and Yashiro, T. (2007). "Seasonal patterns of egg production in field colonies of the termite *Reticulitermes speratus* (Isoptera: Rhinotermitidae)," *Population Ecology* 49(2), 179-183. https://doi.org/10.1007/s10144-0060030-4

Nakayama, T., Yoshimura, T., and Imamura, Y. (2004). "The optimum temperature-humidity combination for the feeding activities of Japanese subterranean termites," *Journal of Wood Science* 50, 530-534.

Smythe, R. V., and Williams, L. H. (1972). "Feeding and survival of two subterranean termite species at constant temperatures," *Annals of the Entomological Society of America* 65(1), 226-229.

Su, N. Y., Mullins, A., and Chouvenc, T. (2023). "Elimination of structural and tree infestations of the Asian subterranean termite with noviflumuron baits in above-ground stations," *Journal of Economic Entomology* 116(3), 909-915.

Takata, M., Konishi, T., Nagai, S., Wu, Y., Nozaki, T., Tasaki, E., and Matsuura, K. (2023). "Discovery of an underground chamber to protect kings and queens during winter in temperate termites," *Scientific Reports* 13, article 8809. https://doi.org/10.1038/s41598-023-36035-1

Tsunoda, K., Matsuoka, H., and Yoshimura, T. (1998). "Colony elimination of *Reticulitermes speratus* by bait application and the effect on foraging territory," *Journal of Economic Entomology* 91(6), 1383-1386. https://doi.org/10.1093/jee/91.6.1383

Article submitted May 21, 2026; Peer review completed: June 17, 2026; Revised version received: June 19, 2026; Accepted: July 5, 2026; Published: July 17, 2026.
DOI: 10.15376/biores.21.3.8350-8365